ISSN1392-1207.MECHANIKA. 2018 Volume24(5): 734-740

LQR and PID Algorithms for Vibration Control of Piezoelectric Composite Plates

Madjid EZZRAIMI*, Rachid TIBERKAK*, Abdelkader MELBOUS, Said RECHAK*****
**Structures laboratory, Mechanical engineering Department, University Blida1, Blida, Algeria, E-mail: ezzmad@yahoo.fr*
***Mechanical engineering Department, University Blida1, Blida, Algeria, E-mail: melbsaek@yahoo.com*
****Laboratory of Mechanical Engineering and Development, Ecole Nationale Polytechnique, Algiers, Algeria, E-mail: said.rechak@enp.edu.dz*

crossref http://dx.doi.org/10.5755/j01.mech.24.5.20645

1. Introduction

The piezoelectricity is used to control the dynamic behavior of structures in order to attenuating vibrations, avoid the resonance and consequently the damage at a later. Active vibration control of composite structures using piezoelectric sensors and actuators has received much attention in several research studies. The dynamic behavior of composite laminate plates has been studied in terms of analytical, numerical and experimental works.

Authors Crawley et al [1, 2] studied the analytic and experimental development of piezoelectric actuators as elements of intelligent structures, where static and dynamic analytic models are derived for segmented piezoelectric actuators that are either bonded to an elastic substructure or embedded in a laminated composite. But in the second paper [2] the development and experimental verification of the induced strain actuation of plate components of an intelligent structure is presented. Dimitradis et al [3] studied the behavior of two dimensional patches of piezoelectric material bonded to the surface of elastic distributed structures and used as vibration actuators is analytically investigated, and the theory is then applied to develop an approximate dynamic model for the vibration response of a simply supported elastic rectangular plate. Her et al [4] present the analytical solution of the flexural displacement of a simply supported plate subjected to the bending moment is solved by using the plate theory, and the effects of the size and location of the piezoelectric actuators on the response of a plate are presented through a parametric study. In [5] Hwang et al presented a finite element formulation for vibration control of a laminated plate with piezoelectric sensors/actuators, and for a laminated plate under the negative velocity feedback control, the direct time responses are calculated by the Newmark-β method, and the damped frequencies and modal damping ratios are derived by modal state space analysis. A finite element method based on the classical laminated plate theory is developed for the active vibration control of a composite plate containing distributed piezoelectric sensors and actuators by Lam et al [6], and the static analysis and active vibration suppression of a cantilever composite plate are performed as a numerical example to verify the proposed model. Liu et al [7] use a simple negative velocity feedback control algorithm coupling the direct and converse piezoelectric effects to actively control the dynamic response of an integrated structure through a closed control loop. Wang et al in [8, 9], studied in the first paper the vibration control of the smart piezoelectric composite plates using the classical negative velocity feedback control method, but in the second one the dynamic stability of the negative velocity feedback control of the composite plate is investigated, so the Lyapunov's energy functional based on the derived general governing equation of motion with active damping is used to carry out the stability analysis. Ang et al [10] propose the use of the total weighted energy method to select the weighting matrices of the linear quadratic regulator (LQR) used to vibration control of smart piezoelectric composite plates. Also Narwal [11] proposed the LQR controller to attenuate the global structural vibration for a simple supported plate structure, and settling time for each different location of piezoelectric patch location was observed which was then followed by an interpretation for the optimal location for piezoelectric patch for maximizing the vibration control. In [12], Bendine et al studied the modeling and active vibration control of a functionally graded (FGM) plate with upper and lower surface bonded piezoelectric layers using the software ANSYS.

Zhang et al in [13], an electro-mechanically coupled finite element (FE) model of smart structures is developed, and considering the vibrations generated by various disturbances, which include free and forced vibrations, a PID control is implemented to damp both the free and forced vibrations. Additionally, an LQR control is applied for comparison, where only total piezoelectric layers are used. Hence exploring patches (partial recovery of piezoelectric layers) and their optimal positions is an important aspect, object of the present paper. The PSO (Particle Swarm Optimization) algorithm to optimize the LQR's parameters is also conducted in this work.

A static deflection control of clamped composite plate by applying various voltages on the actuators is undertaken, and the active control analysis using LQR and PID controllers for attenuating free and forced vibrations has been studied and compared as well.

2. Theoretical formulation

Let us consider a thick composite plate equipped with a piezoelectric layer as show in Fig.1. The composite plate of thickness h and composed of n arbitrarily layers, in which each lamina may be oriented at an angle θ with respect to the x-axis of the coordinate system.

The displacement filed corresponding to Mindlin's hypotheses as a first order shear deformation (FOSD), as follows:

$$\{U\}=\begin{Bmatrix}U\\V\\W\end{Bmatrix}=\begin{bmatrix}1&0&0&-z&0\\0&1&0&0&-z\\0&0&1&0&0\end{bmatrix}\begin{Bmatrix}u\\v\\w\\\theta_x\\\theta_y\end{Bmatrix}=$$

$$=[T]=\{u\}, \tag{1}$$

where: u, v and w denote the mid-plane displacements, θ_x and θ_y denote the rotations along the x and y axis, respectively.

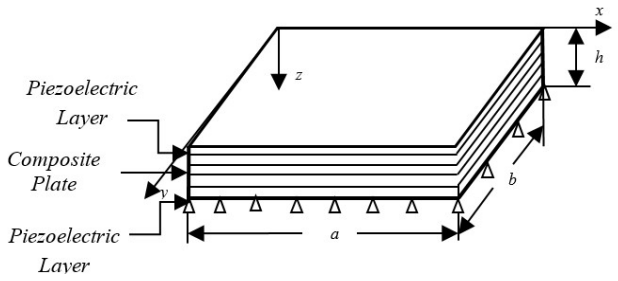

Fig. 1 Description of laminate plate equipped with a piezoelectric element

For a piezoelectric material polarized in the direction of thickness (z), the behavior laws are:

The direct effect of the piezoelectric is done:

$$\{D\}=[e]\{\varepsilon\}+[d]^T\{E\}, \tag{2}$$

where: $\{D\}$ is the vector of electric displacements, $\{\varepsilon\}$ is the deformation vector, $\{E\}$ is the vector of electric fields, $[e]$ is the matrix of piezoelectric constants and $[d]$ is the electrical permittivity matrix.

For the converse effect of the piezoelectric:

$$\{\sigma\}=[C]\{\varepsilon\}-[e]^T\{E\}, \tag{3}$$

where: $\{\sigma\}$ is the constraints vector and $[C]$ is the elastic constants matrix.

The electrical field E is the gradient of the electrical potential ϕ. E is constant along the thickness h_p of the piezoelectric layer:

$$E_Z=-\frac{\phi}{h_p}. \tag{4}$$

The kinetic energy has the same form of a purely elastic layer:

$$E_c=\frac{1}{2}\rho\int\left[\dot{U}\right]^T\left[\dot{U}\right]dv. \tag{5}$$

However, the potential energy has two additional terms:

$$E_c=\frac{1}{2}\int\{\varepsilon\}^T[C]\{\varepsilon\}\,dv-$$
$$-\frac{1}{2}\left(\int\{\varepsilon\}^T[e]\{E\}\,dv+\int\{E\}^T[e]\{\varepsilon\}\,dv\right)-$$
$$-\frac{1}{2}\int\{E\}^T[d]\{E\}\,dv=$$
$$=E_{Elastic}+E_{Piezoelectric}+E_{Dielectric}. \tag{6}$$

3. Finite element discretization

A quadratic finite element with 9 nodes is used. Each node has five degrees of freedom (u, v, w, Θ_x, Θ_y) in addition to an electrical degree of freedom (ϕ). Where:

$$\{u\}=[N_u]\{\bar{u}\}, \tag{7}$$

$$\{\phi\}=[N_\phi]\{\bar{\phi}\}. \tag{8}$$

where: $\{\bar{u}\}$ and $\{\bar{\phi}\}$ are the vectors of nodal displacements and nodal potentials, respectively. $[N_u]$ and $[N_\phi]$ are the interpolation matrices of displacements and electric potentials.

For a piezoelectric multilayer plate, the elementary mass matrix is:

$$[M]_e=\sum_i\rho\int_s[N_u]^T[\bar{m}_e][N_u]\,ds. \tag{9}$$

And, the elementary stiffness matrix is:

$$[K_{uu}]_e=\sum_i h_i\int_s[N_u]^T[D_{uu}]^T[C_{mf}][D_{um}][N_u]\,ds+$$
$$+\sum_i\left(\frac{h_i^3}{12}+z_ih_i\right)\int_s[N_u]^T[D_{uf}]^T[C_{mf}][D_{uf}][N_u]\,ds-$$
$$-\sum_i(z_ih_i)\int_s[N_u]^T[D_{um}]^T[C_{mf}][D_{uf}][N_u]\,ds-$$
$$-\sum_i(z_ih_i)\int_s[N_u]^T[D_{uf}]^T[C_{mf}][D_{um}][N_u]\,ds+$$
$$+\sum_i(kh_i)\int_s[N_u]^T[D_{uc}][C_c][D_{uc}][N_u]\,ds. \tag{10}$$

With z_i is the position of the average plane of the i^{ime} layer.

$$[K_{u\phi}]_e=-\sum_i h_i\int_s[N_u]^T[D_{um}]^T[e_{mf}][D_\phi][N_\phi]\,ds-$$
$$-\sum_i(z_ih_i)_i\int_s[N_u]^T[D_{uf}]^T[e_{mf}][D_\phi][N\phi]\,ds, \tag{11}$$

where: $[K_{u\phi}]_e=[K_{u\phi}]_e^T$ is the component of the elementary stiffness matrix due to the piezo-mechanical coupling.

While the component of the dielectric matrix is:

$$\left[K_{\phi\phi}\right]_e = -\sum_i h_i \int_s \left[N_\phi\right]^T \left[D_\phi\right]^T [d] \left[D_\phi\right] \left[N_\phi\right] ds. \quad (12)$$

The equation of motion of a piezoelectric plate is obtained by assembly of the elementary equations:

$$\begin{bmatrix} M & 0 \\ 0 & 0 \end{bmatrix} \begin{Bmatrix} \ddot{u} \\ \ddot{\phi} \end{Bmatrix} + \begin{bmatrix} K_{uu} & K_{u\phi} \\ K_{\phi u} & K_{\phi\phi} \end{bmatrix} \begin{Bmatrix} u \\ \phi \end{Bmatrix} = \begin{Bmatrix} F \\ Q \end{Bmatrix}, \quad (13)$$

where: $[M],[K],\{F\}$ and $\{Q\}$ are the mass matrix, stiffness matrix, vector of mechanical loads and vector of electric loads, respectively.

The structural Rayleigh damping is used:

$$[C] = \alpha[M] + \beta[K_{uu}], \quad (14)$$

where: α and β are the Rayleigh coefficients.

Equation (13) can be written as:

$$\begin{aligned} &[M]\{\ddot{u}\} + [C]\{\dot{u}\} + [K]\{u\} = \{F_u\} - [K_{u\phi}]\{\phi_a\} \\ &[K_{\phi u}]\{u\} + [K_{\phi\phi}]\{\phi_s\} = \{0\}, \end{aligned} \quad (15)$$

where: *a* and *s* are, actuator and sensor index, respectively.

4. Active vibration control

4.1. Reduced model

Since our interest is only the first modes of vibrations, a reduced model is used for the first (r) modes, and the modal displacement vector becomes:

$$\{q\}_r = [V]_r^T \{u\}, \quad (16)$$

where: $[V]$ is the matrix of eigenvectors.

Substituting Eq. (16) in (15), we obtain the following decoupled system:

$$\begin{aligned} &\left[\overline{M}_{uu}\right]\{\ddot{q}\}_r + \left[\overline{C}_{uu}\right]\{\dot{q}\}_r + \left[\overline{K}_{uu}\right]\{q\}_r = \\ &= [V]_r^T \{F_u\} - [V]_r^T [K_{u\phi}]\{\phi_a\}, \end{aligned} \quad (17)$$

$$\{\phi_s\} = -\left[K_{\phi\phi}\right]^{-1} [K_{\phi u}][V]_r \{q\}_r. \quad (18)$$

4.2. State space representation

The equation of the decoupled system (17) and (18) can be written in terms of state space as follows:

$$\begin{cases} \{\dot{X}(t)\} = [A]\{X(t)\} + [B]\{u(t)\} \\ \{Y(t)\} = [A]\{X(t)\} \end{cases}, \quad (19)$$

where: $\{X(t)\}$, $\{Y(t)\}$ and $\{u(t)\}$ are the state vector, measure vector (output) and the control vector (input). With:

$$\{X\} = \begin{Bmatrix} q \\ \dot{q} \end{Bmatrix}_r, Y = \phi_s, u = \phi_a. \quad (20)$$

$[A]$, $[B]$ and $[C]$ are the matrix of the system, the matrix of the control and the matrix of output, respectively.

$$[A] \begin{bmatrix} 0 & I \\ -\overline{M}_{uu}\overline{K}_{uu} & -\overline{M}_{uu}\overline{C}_{uu} \end{bmatrix}, \quad (21)$$

$$[B] = \begin{bmatrix} 0 \\ -\overline{M}_{uu} V_r^T K_{u\phi} \end{bmatrix}, \quad (22)$$

$$[C] = \begin{bmatrix} -K_{\phi\phi}K_{\phi u}V & 0 \end{bmatrix}. \quad (23)$$

4.3. Linear Quadratic Regulator (LQR)

The optimal input is reached by minimizing a cost function using the optimal control LQR:

$$J_{LQR} = \frac{1}{2}\int \left(X^T Q X + u^T R u \right) dt, \quad (24)$$

where: *Q*, *R* are the weighting matrix (output) and the control vector (input), respectively.

The control law optimizing J function is given by:

$$u(t) = -K X(t), \quad (25)$$

$$K = R^{-1} B^T P, \quad (26)$$

where: *K* and *P* are the gain matrix of the optimal control and solution matrix of the Riccati equation, respectively.

The Riccati equation is:

$$A^T P + P A^T + Q - P B R B^T P = 0, \quad (27)$$

with: $R = \overline{R}$ and $Q = C^T \overline{Q}\, C$.

So, closed loop of the LQR controller becomes:

$$\begin{cases} \dot{X} = (A - BK) X \\ Y = C X \end{cases}. \quad (28)$$

The LQR controller is shown in Fig. 2.

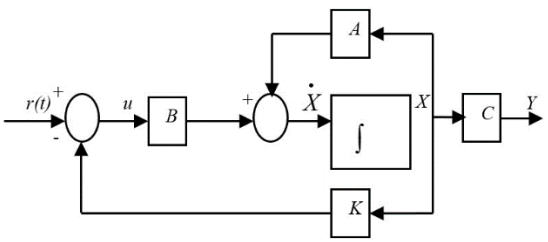

Fig. 2 LQR controller

4.4. Integral-Derived Proportional Regulator (PID)

The PID strategy is to define the control vector u(t) as a summation of the proportional, integral and derivative of the vector of the output error e(t) by:

$$u(t) = K_p e(t) + K_i \int e(t)dt + K_d \frac{de(t)}{dt}, \quad (29)$$

where, the vector of the output error e(t) is given by:

$$e(t) = -Y(t) = -C\,X(t). \quad (30)$$

In Eq. (29) K_p, K_i *et* K_d are the proportional gain, the integral gain and the derivative gain, respectively.

The PID controller is shown in Fig. 3.

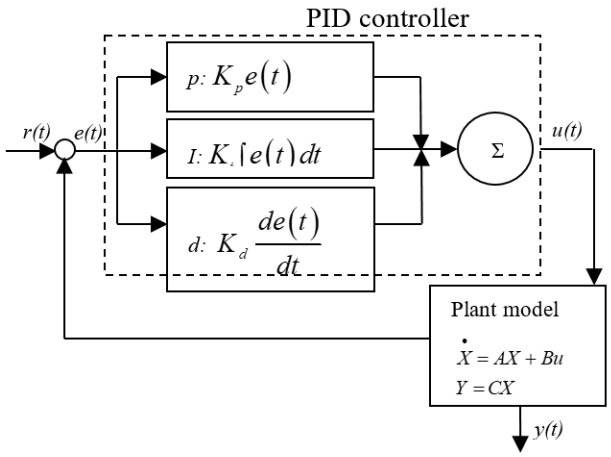

Fig. 3 PID controller by retroaction

5. Numerical results and discussions

In this section, a cantilevered piezolaminated composite plate is studied.

5.1. Verification of numerical model

For this propose, a comparative survey is undertaken in order to check the correctness of the results of the developed program by comparing them with those of the literature.

Table 1

Materials properties

	PZTG1195N	T300/976
Young's Moduli (GPa)		
E_{11}	63.0	150
E_{11}= E_{33}	63.0	9
Poisson's ratio		
ν_{23}	0.3	0.3
ν_{12}= ν_{13}	0.3	0.3
Shear moduli (GPa)		
G_{23}	24.2	7.1
G_{12}=G_{13}	24.2	2.5
Density ρ(kg/m^3)	7600	1600
Piezoelectric constants (m/V)		
d_{31}=d_{32}	254 10^{-12}	
Electrical permittivity (F/m)		
ε_{11}= ε_{22}	15.3 10^{-9}	
ε_{33}	15.0 10^{-9}	

In this section, a sandwich plate 200x200 mm, in which the master layer is made of graphite/epoxy composite (T300/ 976). The configuration of the composite plate is [- 45/45-45/45], with a total thickness of 1 mm, which is situated between two piezoelectric layers (PZT G1195 N) of 0.1mm each. This structure was proposed by LAM et al [6].

The properties of the materials are given in Table. 1.

The first five eigenfrequencies are calculated and presented in Table 2.

Table 2

The first five eigenfrequencies (rad/s)

Mode	LAM et al [6]	Present	Discrepancy (%)
1	21.4657	21.4308	0.16
2	63.3491	63.0758	0.43
3	130.8221	129.1594	1.27
4	182.4224	182.1370	0.15
5	218.2750	216.7596	0.69

As one can see from table 2, that the present results compare well with those presented by LAM et al.

5.2. Static deflection control

In this case, all the piezoceramics on the upper and lower surfaces on the plate are used as actuators.

In first, the two piezoelectric layers completely cover the top and bottom surfaces.

It is noted that the plate is initially exposed to a mechanically uniformly distributed load of 100 Pa.

The deflection of the center line for different potential values is shown in Fig. 4.

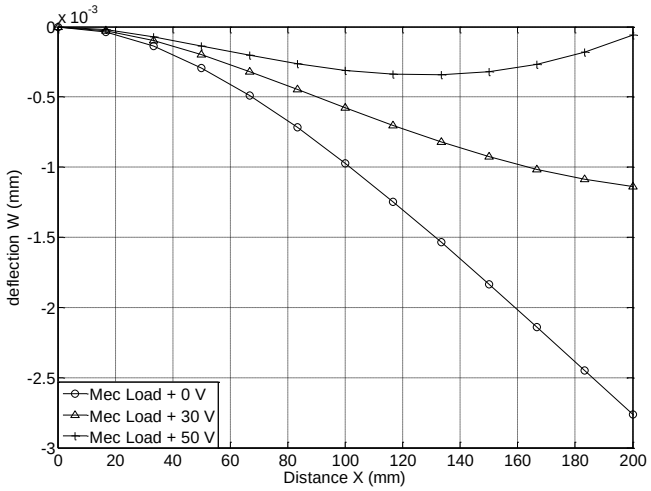

Fig. 4 Deflection of the central line

From Fig. 4, it can be seen that for the control of the deflection, different values of voltages are applied on the actuators. The attenuation is obtained until the desired tolerance for voltage value at 50 V.

Secondly, the same structure is used, but the piezoelectric layers are taken as a patches recovering third of the total surface of the plate (1/3). So to analyze the influence of the position of the patches (actuators) on the control, we test three configurations of patches positions A, B, and C (Fig. 5).

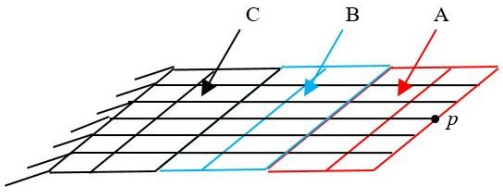

Fig. 5 Patches position A, B, and C

For the same loading condition of 100Pa, the actuators are at 0 v and at 80 v. The deflection *w* of the central line is shown in Fig. 6.

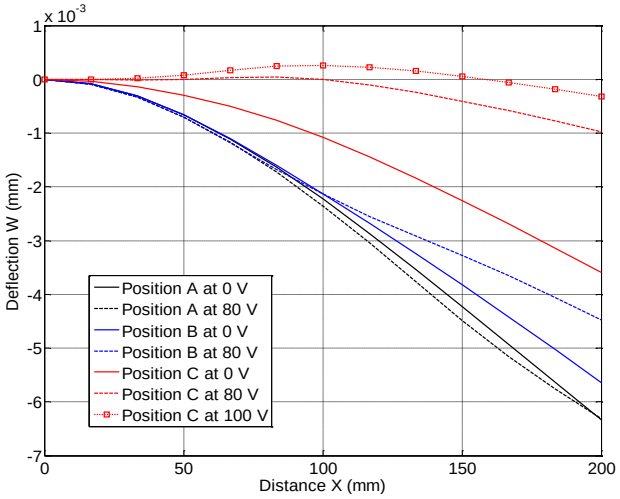

Fig. 6 Deflection of the central line (Patches)

We notice, from Fig.6, that the configuration C has a better results compared to other configurations A and B, but needs more power (80V instead of 50V) to have the same level of attenuation as that of total piezoelectric layer (see Fig.4). Then, the configuration C will be used for the active control in the following section.

5.3. Active control

The control concerns the same structure, but the upper piezoelectric layer acts as a sensor, while the lower one as actuator. Two algorithms LQR and PID for different parameters are used to control vibrations.

In this case the two piezoelectric layers completely cover the upper and lower surfaces of the plate. The structure is excited by a mechanical loading of a step force of 1 N at the P point starting from 0.1 s (P is on the free side of the central line).

For this step, to test the influence of the control parameters on the LQR and PID controller's performance, we used parameters find in article [13] (Table 3). These parameters are optimized by PSO (Particle Swarm Optimization) algorithm to use them in the next application.

Table 3

Control parameters

Control type	$\bar{Q}$	$\bar{R}$	
LQR 1	1/5/5	1/8.8/8.5	
LQR 2	1/5/5	1/70/70	
Control type	K_p	K_i	K_d
PID 1	2	100	0.01
PID 2	2	400	0.03

The sensor and actuator signal as well as deflection of P point are shown in Figs. 7, a, b and c.

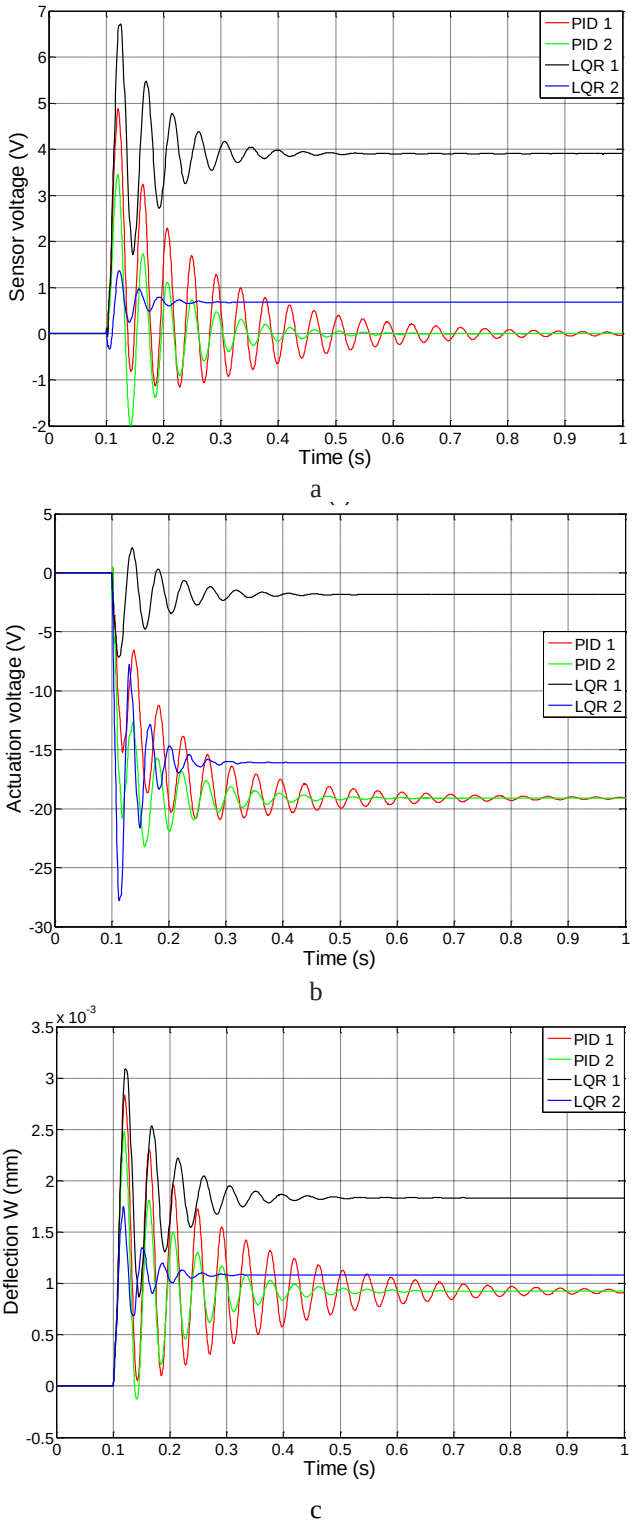

Fig. 7 Dynamic response by LQR and PID controllers under step force excitation

From Fig. 7, we notice that the LQR1 and LQR2 controllers attenuates the free vibrations, but only LQR2 suppress slightly the forced vibrations. Also, one can see that the PID1 and PID2 controllers damp also the free vibrations, and decrease forced vibrations more than LQR2. However, one can remark that PID2 give fast suppression of vibration in short period than the PID1.

In the second application, we take the patches of the configuration C which gave the best results with respect to A and B for the static control (Fig. 6).

The mechanical loading is also a step force of 1 N applied at point P. The PID and LQR controllers are used for active control of forced vibrations, and the control parameters are optimized using PSO algorithm to improve performance of LQR controller. Obtained results are shown in Fig. 8.

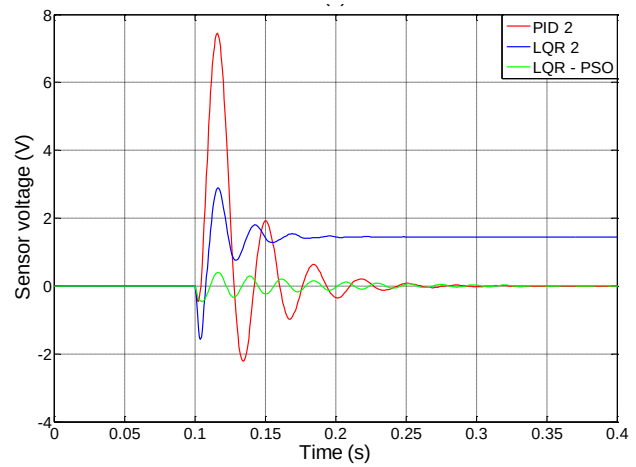

a

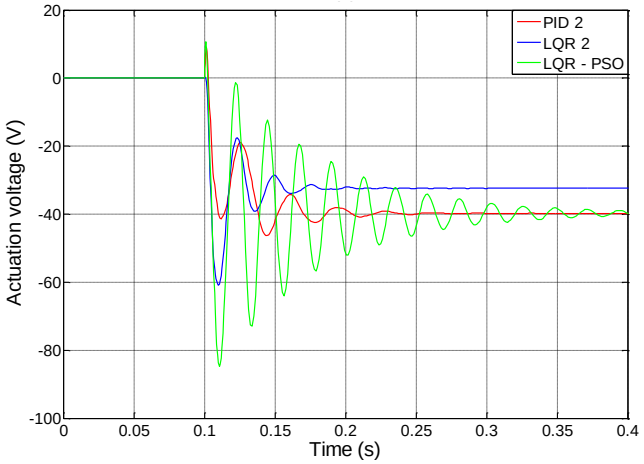

b

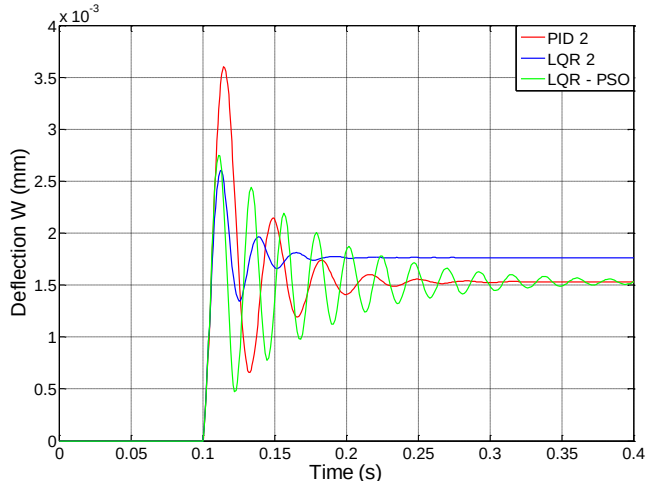

c

Fig. 8 Dynamic response by LQR and PID controllers under step force excitation (Patches)

The parameters of LQR2 and PID2 are given in Table 3, while those of LQR-PSO are calculated by the PSO algorithm:

$$\bar{Q} = 1.528914266394741e\text{-}001,$$
$$\bar{R} = 2.373296423061706e\text{-}005.$$

From Fig. 8, one can see that:

(*i*) The same observations are made concerning the successful attenuation of free and forced vibrations using patches compared to those using total piezoelectric layers.

(*ii*) We also notice that the performances of the patches in configuration C are almost as good as those of the case of total piezoelectric layers despite a ratio of the surfaces patches which is 1/3, but use more power for the control (40 V) compared with (20 V).

(*iii*) The PID2 controller attenuate the forced vibrations better than the LQR2, but using the LQR's parameters (LQR-PSO) optimized by PSO algorithm has given the same performances compared to those of the PID2 controller.

6. Conclusion

A composite plate incorporating piezoelectric elements has been tested for static and dynamic vibration control using finite element model.

Firstly, a static analysis exploiting the actuators for the attenuation of the vibrations is conducted. Then different configurations of patches A, B and C were tested to obtained the optimal patch location.

Secondly, the active control with the LQR and PID controllers was studied. The two types of controllers (LQR and PID) suppress the free vibrations with success but with the ascendant of the second (PID) over the period of the attenuation.

On the other hand, for the forced vibrations the performances of PID are best compared to the LQR, but the optimized LQR's parameters using PSO algorithm can give the same performances as the PID controller. We also notice that the performances of the patches in configuration C are almost as good as those of the total piezoelectric layers despite a ratio of the surfaces patches which is 1/3, but the configuration C use more power for the control.

References

1. **Crawley, E. F.; de Luis, J.** 1987. Use of piezoelectric actuators as elements of intelligent structures, AIAA Journal, 25(10):1373-1385. https://doi.org/10.2514/3.9792.
2. **Crawley, E. F.; Lazarus, K. B.** 1991. Induced strain actuation of isotropic and anisotropic plates, AIAA Journal, 29(6):944-951. https://doi.org/10.2514/3.10684.
3. **Dimitriadis, E. K.; Fuller, C. R.; Rogers, C. A.** 1991. Piezoelectric actuators for distributed vibration excitation of thin plates, Journal of Vibration and Acoustics, 113:100-107. https://doi.org/10.1115/1.2930143.

4. **Her, S. C.; Liu, C. Y.** 2007. The deflection of a simply supported plate induced by piezoelectric actuators, Journal of Mechanical Science and Technology, 21: 1745-1751. https://doi.org/10.1007/BF03177404.
5. **Hwang, W. S.; Park, H. C.** 1993. Finite element modeling of piezoelectric sensors and actuators, AIAA Journal, 31(5): 930-937. https://doi.org/10.2514/3.11707.
6. **Lam, K. Y.; Peng, X. Q.; Liu, G. R.; Reddy, J. N.** 1997. Finite element model for piezoelectric composite laminates, Smart Mater. 6: 583-591. https://doi.org/10.1088/0964-1726/6/5/009.
7. **Liu, G. R.; Penk, X. Q.; Lam, K. Y.; Tani, J.** 1999. Vibration control simulation of laminated composite plates with integrated piezoelectrics, Journal of Sound and Vibration, 220(5), 827-846. https://doi.org/10.1006/jsvi.1998.1970.
8. **Wang, S. Y.; Quek, S. T.; Ang, K. K.** 2001. Vibration control of smart piezoelectric composite plates, Smart Materials and Structures 10 (4): 637-644. https://doi.org/10.1088/0964-1726/10/4/306.
9. **Wang, S.Y.; Quek, S.T.; Ang, K.K.** 2004. Dynamic stability analysis of finite element modeling of piezoelectric composite plates, International Journal of Solids and Structures, 41: 745–764. https://doi.org/10.1016/j.ijsolstr.2003.09.041.
10. **Ang, K. K.; Wang, S. Y.; Quek, S. T.** 2002. Weighted energy linear quadratic regulator vibration control of piezoelectric composite plates, Smart Materials and Structures, 11: 98-106. https://doi.org/10.1088/0964-1726/11/1/311.
11. **Narwal, K.; Chhabra, C.** 2012. Analysis of simple supported plate for active vibration control with piezoelectric sensors and actuators, IORS Journal of Mechanical and Civil Engineering 1(1): 26-39. https://doi.org/10.9790/1684-0112639.
12. **Bendine, K.; Boukhoulda, B. F.; Nouari, M.; Satla, Z.** 2017. Structural modeling and active vibration control of smart FGM plate through ANSYS, International Journal of Computational Methods 14(2): 1750042. https://doi.org/10.1142/S0219876217500426.
13. **Zhang, S.; Schmidt, R.; Xiansheng, Q.** 2015. Active vibration control of piezoelectric bonded smart structures using PID algorithm, Chinese journal of aeronautics, 28 (1), 305-313. https://doi.org/10.1016/j.cja.2014.12.005.

M. Ezzraimi, R. Tiberkak, A. Melbous, S. Rechak

LQR AND PID ALGORITHMS FOR VIBRATION CONTROL OF PIEZOELECTRIC COMPOSITE PLATES

S u m m a r y

In this paper, a formulation of a sandwich plate integrating an elastic central layer (isotropic or composite) between two piezoelectric layers (actuators and/or sensors), which can be taken as a smart (intelligent) structure and allowing active control vibrations is presented. A 9-node finite element quadratic plate element with 5 degrees of freedom per node is used which takes into account the effect of transverse shear with an additional degree of freedom for each node of the piezoelectric layer.

At first, the static control of the deflection by taking the two piezoelectric layers as actuators with two configurations of the total piezoelectric layer and patches is undertaken. Thus, the influence of patches position, for the second configuration, on the attenuation of vibrations is analyzed.

In a second step, the active vibration control using two types of LQR and PID controllers with different control parameters is tested and compared for the two configurations (total piezoelectric layer and patches). It is demonstrated throughout the present results that the performances of the patches are almost as good as those of the total layer despite a ratio of the surfaces patches which is 1/3. It is also noticed that the PID controller is more efficient than the LQR controller. But, if using the PSO (Particle Swarm Optimization) algorithm, the LQR's parameters are optimized and give almost the same performances as those of the PID controller.

Key words: finite element method, composite plates, vibrations, piezoelectric, active control, LQR, PID, PSO.

Received April 23, 2018
Accepted October 18, 2018